BBA 46189

THE TWO-IRON FERREDOXINS IN SPINACH, PARSLEY, PIG ADRENAL CORTEX, *AZOTOBACTER VINELANDII*, AND *CLOSTRIDIUM PASTEURIANUM*: STUDIES BY MAGNETIC FIELD MÖSSBAUER SPECTROSCOPY*

W. R. DUNHAM AND ALAN J. BEARDEN

Donner Laboratory, University of California, Berkeley, Calif. 94720 (U.S.A.)

I. T. SALMEEN**, G. PALMER AND R. H. SANDS

Biophysics Research Division, Institute of Science and Technology, University of Michigan, Ann Arbor, Mich. 48105 (U.S.A.)

W. H. ORME-JOHNSON AND H. BEINERT

Department of Biochemistry and the Institute for Enzyme Research University of Wisconsin, Madison, Wisc. 53706 (U.S.A.)

(Received May 21st, 1971)

SUMMARY

The two-iron ferredoxins from spinach, parsley, *Azotobacter vinelandii*, *Clostridium pasteurianum* and the pig adrenal cortex were investigated by Mössbauer spectroscopy at temperatures from 4 to 256°K and in magnetic fields up to 46 kGauss. Computational programs were devised to allow comparison of the experimental data with computer-simulated spectra in order to facilitate identification of the experimental spectral detail with specific Mössbauer spectroscopic parameters (quadrupole splittings, isomer shifts and nuclear hyperfine and nuclear Zeeman interactions). The results of the analysis permit the following properties of the active center to be established directly as the result of these experiments:

1. In the oxidized forms of the proteins, each iron is in the high spin ($S = 5/2$) ferric state, spin-coupled to produce a resultant molecular diamagnetism for the protein at temperatures below 100°K.

2. In the reduced state of the protein, the active center contains a single ferric site, retaining many properties of the ferric iron in the oxidized protein, but spin-

Abbreviation: ENDOR, electron–nuclear double resonance.

* This is one of a series of papers describing the electronic properties of spinach ferredoxin and other iron–sulfur proteins; related publications contain the results of experiments on the electron–nuclear double resonance (called I)[9], magnetic susceptibility (called III)[10] and infrared, optical and circular dichroism (called IV)[12] spectra. An integrated interpretation of all our data in terms of a specific model for these proteins will be published separately. The work reported in this paper (called II) and that reported in I was first presented at the 4th International Conference on Magnetic Resonance in Biological Systems, Oxford, August, 1970 (R. H. SANDS, J. FRITZ, A. BEARDEN AND W. R. DUNHAM).

** Present address: Scientific Research Staff, Ford Motor Company, Dearborn, Mich. 48121, U.S.A.

coupled to a high spin ($S = 2$) ferrous site, producing a molecular paramagnetism due to a net electron spin of one half at low temperatures ($S = 1/2$).

3. In spinach and parsley ferredoxins, the ligand symmetry around the ferrous site in the reduced form of the proteins is tetrahedral with measurable axial and rhombic distortions.

4. The iron sites in both the oxidized and reduced forms of all the proteins studied are similar, with the possible exception that the ligand symmetry at the ferrous site in the reduced form of the two-iron ferredoxins from *C. pasteurianum*, *A. vinelandii* (Azotobacter I and II), and pig adrenal cortex has not been characterized as being square planar or tetrahedral, although octahedral symmetry has been excluded.

INTRODUCTION

The "two-iron ferredoxins" are intracellular electron-transfer proteins which contain a two-iron, two acid-labile sulfur complex at their active centers. These proteins function in a variety of biochemical pathways[1-3] and in all cases, the addition of a single electron to the oxidized form of the proteins provides the reduced form of these proteins, which are strong reducing agents with reduction potentials from —250 to —420 mV. Since the reducing electron has been located at the iron–sulfur complex by electron paramagnetic resonance (EPR) experiments[4-8], we are led to the application of ^{57}Fe Mössbauer spectroscopy in the study of the active centers of these "two-iron ferredoxins". In this paper, Mössbauer spectroscopic data are presented for six proteins: parsley and spinach (PPNR) ferredoxin, adrenodoxin, Azotobacter iron–sulfur proteins I and II, and the *Clostridium pasteurianum* paramagnetic protein. These data, when coupled to data obtained by EPR, electron–nuclear double resonance (ENDOR)[9], magnetic susceptibility[10,11] and near infrared studies[12], permit characterization of the iron environment at the active center of these proteins. The questions amenable to study by Mössbauer spectroscopy are: (1) what are the oxidation and spin states of the iron in both the oxidized and reduced forms of the two-iron ferredoxins and (2) what is the degree of covalency and the coordination geometry of the ligands surrounding each iron atom.

To answer these questions, Mössbauer spectra of ^{57}Fe-enriched proteins taken under a wide range of temperature and magnetic field conditions are presented for the oxidized and reduced forms of these proteins. In order to extract parameters useful in providing answers to these questions, computer-simulated Mössbauer spectra are compared with the experimental data until a set of "best fits" are realized; further discussion then proceeds using these Mössbauer spectroscopic parameters.

MATERIALS AND METHODS

Because Mössbauer spectroscopy requires the presence of ^{57}Fe nuclei in order to sense the small perturbations of nuclear energy levels produced by the surrounding electronic environments, better signal-to-noise conditions can be realized by enriching the protein with ^{57}Fe well above the 2.19 % natural isotopic abundance. All proteins were enriched to 80–90 % in ^{57}Fe *via* published chemical exchange procedures; the

material after exchange being characterized by optical spectroscopy and observation of the EPR signal in the reduced state. The first paper[9] in this series describes ENDOR experiments on "two-iron ferredoxins". Since ^{57}Fe-enriched proteins in the ENDOR experiments are identical to those in our own studies, we refer the reader to that paper for the details of the preparation of the proteins from spinach, parsley and pig adrenal cortex.

The proteins from Azotobacter were purified and the iron exchanges carried out as described by DERVARTANIAN *et al.*[13]. The clostridium paramagnetic protein was isolated as described by HARDY *et al.*[14] with the addition of a final electrophoresis step as described for adrenodoxin[15]. The iron exchange was also carried out as described for adrenodoxin[6–8]. In each case the extent of replacement of ^{56}Fe with ^{57}Fe was monitored with added ^{59}Fe. The final enrichment in ^{57}Fe was approximately 90 %.

The products of these ^{57}Fe reconstitution experiments are indistinguishable from the native proteins by optical and CD spectroscopy and by activity measurements[16], though the introduction of the ^{57}Fe does affect the EPR spectrum in the reduced state by means of the hyperfine interaction between the iron nuclei and the net electronic spin. No extraneous iron can be detected in the reconstituted and purified proteins.

Spinach and parsley ferredoxin do not suffer any detectable deterioration on one cycle of lyophilization[10,11,17]. Whereas no previous data is available for adrenodoxin, the Mössbauer spectrum from the lyophilized material was identical to that from the frozen aqueous solution; this would imply that the lyophilization does not appreciably affect this protein either. Only the spinach and adrenodoxin proteins were lyophilized in this study.

The dithionite-reduced proteins can be frozen and thawed several times without any measurable changes in the EPR spectra, and since the EPR spectrum is recognized as a physical assay for these proteins[18] this indicates that negligible deterioration results. For the experiments reported here the samples, once frozen in the reduced state, were never allowed to thaw; thus the slight deterioration (approx. 5 %) which is known to occur on reoxidation[19] was avoided. The Mössbauer spectra were repeated at the initial temperature employed in each study and no deterioration due to temperature cycling or radiation was detected.

Mössbauer samples were 0.3 ml of 2–6 mM aqueous solution (1–2 μmoles of protein), buffered anaerobically with 0.1 M Tris chloride, pH 7.5–8, placed in a polyethylene cuvette and stored in liquid nitrogen. Reduction of the samples, when required, was effected by the addition of solid sodium dithionite to the aqueous solution of the oxidized proteins (the adrenal protein solution was 10 μM in methyl viologen[15]); these procedures were performed directly in the Mössbauer cuvette using a stream of ^{4}He gas to thaw the sample and to mix the reductant anaerobically. After a 5-min equilibration period, the sample cuvette was placed in liquid nitrogen and then reassembled into the Mössbauer spectrometer dewar system without subsequent thawing of the sample. In several cases where lyophilization of the sample seemed appropriate this was accomplished directly in the Mössbauer cuvette.

There are two design features of the Mössbauer cuvette[20] which were essential because spectra must be taken at known sample temperatures between 4.2°K and the ice point: (1) ^{4}He exchange gas was present in the cuvette to equilibrate the sample temperature with the walls and with a carbon resistor resistance thermometer, and

(2) with a heater wound on its outer diameter the cuvette was placed in loose thermal contact with the inner bore of a copper tube whose exterior was surrounded by liquid ^{4}He. ^{4}He exchange gas was introduced inside the copper tube at pressures ranging between 10 and 10^{-3} torr depending on the degree of thermal contact desired with the liquid helium bath. These features allowed the sample temperature to be known and regulated within 0.1 to 1°K over the temperature range from 4.2 to 256°K. The resistance thermometer was a 0.125-W, 1500-Ω carbon composition resistor. The heater power was electronically regulated to maintain the sample temperature during the ten to twenty hours of a typical Mössbauer run.

Magnetic fields of up to 50 kGauss were applied parallel to the γ-ray observation direction by means of a superconducting solenoid (Westinghouse Research and Development), the magnetic field determination being made by measuring the current supplied to the magnet from a regulated current source and the known geometry and turns number of the solenoid. The superconducting solenoid was operated in a non-persistent mode using gas-cooled leads from the helium dewar in order to permit continuous monitoring of the field during a run.

The Mössbauer spectrometer used a constant-acceleration cam which was a variant of a cam system previously described[21]. The Mössbauer sources used were ^{57}Co:Pt with source strengths from 50 down to 20 mC and displayed linewidths (FWHM) of 0.27 mm/sec with thin natural enrichment absorbers of $Na_4Fe(CN)_6 \cdot 10\ H_2O$. A multichannel scaler (RIDL 34-8) stored data (counts per channel) *vs.* source velocity, receiving discriminator pulses from a single channel analyzer at the output of a two-unit pulse amplifier recording the output of a Xe–N_2 (95:5, v/v) gas-filled proportional counter. The multichannel scaler data were transferred to temporary magnetic storage after each hour of running. When a run was complete the data were transferred to punched cards; a computer plot program furnished a plot of "percent absorption" *vs.* "source velocity". This plot was corrected for the varying source-to-counter distance at each velocity and for the absorption (approx. 0.2 %) from small amounts of iron in the counter window.

The dewar assembly was constructed to minimize both the source-to-counter distance (to ensure high counting rates) and helium boiloff[20]. A single filling of liquid ^{4}He permitted operation of the dewar for about 6 h with the highest sample temperature (225°K) and the maximum magnetic field (50 kGauss).

The spectrometer reproduced detail to 0.002 mm/sec on the velocity axis; the percent absorption accuracy was determined only by counting statistics.

COMPUTATIONAL METHODS

Mössbauer spectroscopic data contain a wealth of information on the detailed electronic configuration in the vicinity of the ^{57}Fe nuclide; these data can be summarized in terms of several spectroscopic parameters: the isomer shift (I.S.) relative to a standard, the quadrupole splitting parameters, and the nuclear hyperfine interaction and Zeeman parameters[22]. Due to the complexity of Mössbauer spectra caused by the amorphous nature of the sample, it is desirable to produce calculated spectra for these parameters in combination and then to adjust the parameters in the calculations until a "best-fit" is made with the experimental data. As energy modulation in Mössbauer spectroscopy is provided *via* a relativistic Doppler shift,

the energy scale is given in terms of relative velocity between source and absorber; hence 1 mm/sec = $4.8075 \cdot 10^{-8}$eV = $3.8778 \cdot 10^{-4}$ cm^{-1} = 11.625 MHz for 14.4-keV γ-rays.

The calculations for these investigations are based on the spin Hamiltonian for ^{57}Fe nuclei coupled to a net electronic spin and in an applied magnetic field[19].

$$\mathscr{H} = \text{I.S.} + \mathscr{H}_{\text{quad}} + \langle \widetilde{S_{\text{eff}}} \rangle \cdot \overset{\approx}{A} \cdot \tilde{I} - g_n \beta_n H I_z \qquad (1)$$

where I.S. is the isomer shift caused by the electrostatic interaction of the nucleus with the total electron charge density inside the nucleus and can be determined by moving the entire computed spectrum along the energy axis (velocity axis) to make it correspond to the experimental data. $\mathscr{H}_{\text{quad}}$ is the part of the spin Hamiltonian resulting from the nuclear quadrupole moment of the ^{57}Fe ($I = 3/2$) excited state interacting with the electric field gradient ($\overset{\approx}{\nabla} E$) at the nuclear position produced by the external charges and is given by,

$$\mathscr{H}_{\text{quad}} = 2DI_z^2 + (E - D)I_x^2 + (-E - D)I_y^2 \qquad (2)$$

where $D = \text{Q.S.}/(6(1 + \eta/3)^{1/2})$, $E = \eta D$ and Q.S. is the observed splitting of a quadrupole pair when the magnetic field at the nuclear position is zero. $I_{x,y,z}$ are the components of the nuclear spin ($I = 1/2$ for the ground state of ^{57}Fe and $I = 3/2$ for the 14.4 keV first excited state of ^{57}Fe). $\langle \widetilde{S_{\text{eff}}} \rangle \cdot \overset{\approx}{A} \cdot \tilde{I}$ is the hyperfine interaction with the net electron spin $\langle \widetilde{S_{\text{eff}}} \rangle$, the latter being quantized in space by the anisotropic electron Zeeman interaction ($-\tilde{H} \cdot \overset{\approx}{G} \cdot \tilde{S}$); the last term in the Hamiltonian represents the interaction of the nuclear moments with the applied magnetic field H_z.

The calculated spectra shown here are the output of a FORTRAN program (ANIMO) written by one of the authors (W.R.D.). This program and a discussion of its use in ^{57}Fe Mössbauer spectroscopy is available[20]. It is capable of calculating Mössbauer spectra for ^{57}Fe with the following restrictions: all calculations are in terms of stationary states, the G- and A-tensors are assumed to be coaxial, and no account of variation in recoil-free fraction from the Goldanskii–Karyagin Effect[23] or thick absorber effects is included. These limitations do not affect the application to the study here presented. A second Mössbauer program was developed independently by one of us (I.T.S.) which, in addition to the above, permits the arbitrary rotations of all three tensors ($\overset{\approx}{G}$, $\overset{\approx}{A}$, $\overset{\approx}{\nabla} E$). We used this program to show that the computed spectra shown here are insensitive to the relative orientation of the G- and A-tensors and also insensitive to small differences in the relative orientation of the $\overset{\approx}{\nabla} E$-tensor. Large reorientation of $\overset{\approx}{\nabla} E$ are handled by axis interchanges in ANIMO.

RESULTS

Oxidized proteins

Mössbauer spectra at 4°K of the oxidized forms of spinach (PPNR) and parsley ferredoxin, clostridial paramagnetic proteins, adrenodoxin, and the two proteins (I and II) from Azotobacter in the absence of applied magnetic field are shown in Fig. 1. Data taken at 77°K are similar to the data taken at the lower temperature, except for a change in the recoil-free fraction resulting in a reduced Mössbauer

absorption, the quadrupole splitting is nearly temperature independent. Spectra obtained at 4°K for the oxidized forms of the proteins (except parsley ferredoxin) with 46 kGauss magnetic field applied along the γ-ray observation direction are shown in Fig. 2.

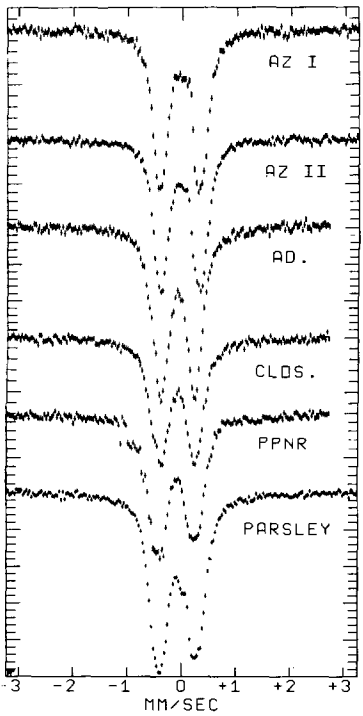

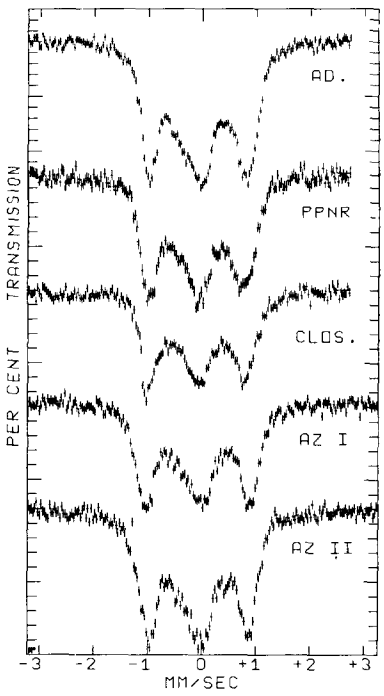

Fig. 1. Mössbauer spectra of the oxidized proteins at 4°K and $H = 0$; platinum source matrix. From top to bottom: Azotobacter protein I, Azotobacter protein II, adrenodoxin, Clostridium paramagnetic protein, spinach ferredoxin, parsley ferredoxin.

Fig. 2. Mössbauer spectra of the oxidized proteins at 4°K and $H = 46$ kGauss; platinum source matrix; H parallel to the γ-ray direction. From top to bottom: adrenodoxin, spinach ferredoxin, Clostridium paramagnetic protein, Azotobacter protein I, Azotobacter protein II.

The Mössbauer spectra of the oxidized forms of the proteins shown in Fig. 1 and 2 may be characterized by a single quadrupole pair and the absence of an observable hyperfine field. Thus both iron atoms per molecule are in equivalent or nearly equivalent environments in the oxidized forms of all proteins studied. Table I lists the values of the isomer shift, quadrupole splitting, and the asymmetry parameter, η, which produce the best equivalent-iron fit of the calculated spectra with the experimental data at 4°K; note that within the experimental limits, all of the oxidized proteins display the same Mössbauer parameters. Small differences in these parameters for biological samples may be due to: (1) impurity absorption due to adventitious ^{57}Fe, (2) strain produced in the iron environment due to the freezing operation, (3) small second-order magnetic effects or (4) true slight non-equivalence of the iron sites. Detailed analysis of the data has not permitted any conclusion in regard to the significance of these small differences, although it is to be noted that the linewidth

TABLE I

MÖSSBAUER PARAMETERS FOR THE OXIDIZED PROTEINS AT 4.2 °K

Protein	*I.S./Pt** (*mm/sec*)	*Q.S.* (*mm/sec*)	η
Spinach ferredoxin	$-0.08 \begin{smallmatrix}+0.06\\-0.03\end{smallmatrix}$	$0.65 \begin{smallmatrix}+0.09\\-0.07\end{smallmatrix}$	0.5 ± 0.3
Parsley ferredoxin	$-0.07 \begin{smallmatrix}+0.06\\-0.03\end{smallmatrix}$	$0.66 \begin{smallmatrix}+0.09\\-0.07\end{smallmatrix}$	0.5 ± 0.3
Adrenodoxin	$-0.08 \begin{smallmatrix}+0.06\\-0.03\end{smallmatrix}$	$0.61 \begin{smallmatrix}+0.09\\-0.07\end{smallmatrix}$	0.5 ± 0.3
Clostridium paramagnetic protein	$-0.07 \begin{smallmatrix}+0.06\\-0.03\end{smallmatrix}$	$0.62 \begin{smallmatrix}+0.09\\-0.07\end{smallmatrix}$	0.5 ± 0.3
Azotobacter iron-sulfur protein I	$-0.04 \begin{smallmatrix}+0.06\\-0.03\end{smallmatrix}$	$0.73 \begin{smallmatrix}+0.09\\-0.07\end{smallmatrix}$	0.5 ± 0.3
Azotobacter iron-sulfur protein II	$-0.06 \begin{smallmatrix}+0.06\\-0.33\end{smallmatrix}$	$0.71 \begin{smallmatrix}+0.09\\-0.07\end{smallmatrix}$	0.5 ± 0.3

* Isomer shifts quoted here are given relative to a γ-ray source consisting of ^{57}Co diffused into a platinum matrix.

required to fit the oxidized protein data is considerably larger than the instrumental linewidth (0.30 mm/sec) and this may be indicative of slight nonequivalence in the iron sites. It is to be emphasized, however, that there are other interactions which can be responsible for increased linewidths and therefore no conclusions are possible in regard to the equivalence or slight non-equivalence of the iron sites in the oxidized protein. It can only be concluded that the sites are quite similar if not identical.

Reduced proteins

In contrast to the spectra taken on the oxidized forms of the proteins, Mössbauer spectra of the reduced forms show highly temperature-dependent nuclear hyperfine interactions. At 4°K and in an external field (580 Gauss) strong enough to produce spatial alignment of electron paramagnetic moments in these materials, a nuclear hyperfine interaction is evident (Fig. 3). As the protein temperature is raised from 4 to 185°K, the nuclear hyperfine interaction becomes less evident until at the highest temperature a Mössbauer spectrum consisting of two quadrupole pairs is resolved (the interpretation is detailed in the next section); this temperature dependence is shown for the reduced form of spinach ferredoxin in Fig. 4. Application of 46 kGauss to the reduced proteins at 4°K yields the spectra shown in Fig. 5, the spectral detail has increased and thus affords further opportunity for matching by computer-simulated Mössbauer spectra.

COMPARISON OF EXPERIMENTAL SPECTRA WITH COMPUTER-SIMULATED MÖSSBAUER ABSORPTION CURVES

In order to extract maximum information from the experimental data, a series of computer-simulated Mössbauer absorption curves were obtained for systematically

varied values of the Mössbauer spin-Hamiltonian parameters previously discussed. These simulated curves are normalized to the point of maximum absorption in the experimental spectra. Before looking at such comparisons, it should be pointed out

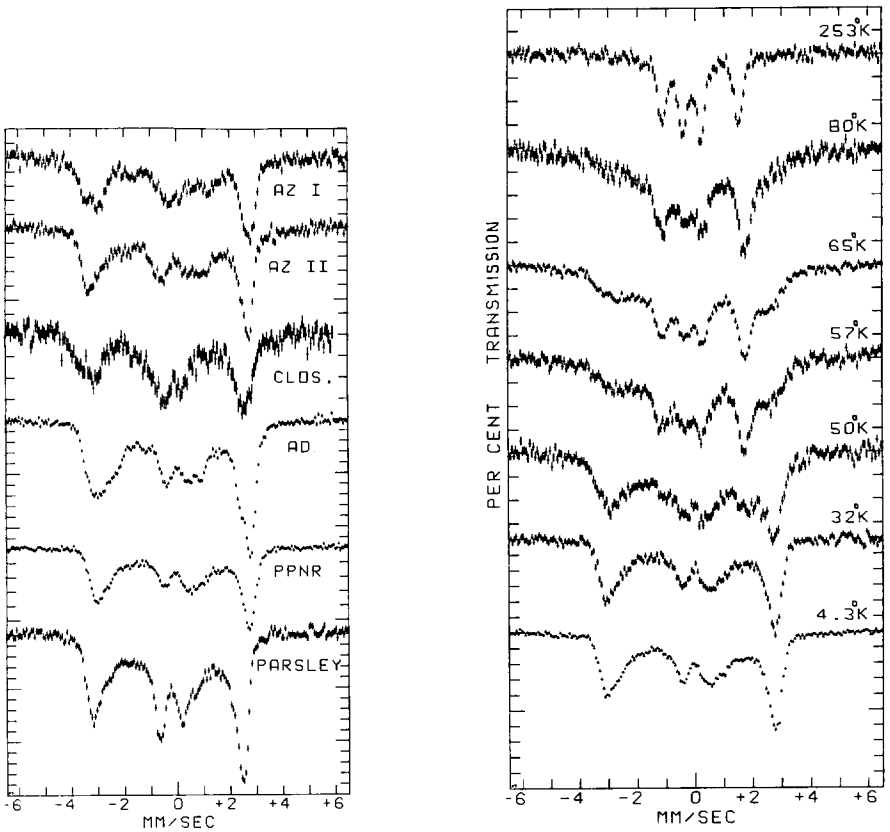

Fig. 3. Mössbauer spectra of the reduced proteins at 4 °K and H = 580 Gauss; platinum source matrix; H parallel to the γ-ray direction. From top to bottom: Azotobacter protein I, Azotobacter protein II, Clostridium paramagnetic protein, spinach ferredoxin, parsley ferredoxin.

Fig. 4. Mössbauer spectra of spinach ferredoxin at temperatures between 4.3 and 253 °K; platinum source matrix; H = 580 Gauss parallel to the γ-ray direction.

that the lability of these proteins makes it difficult to obtain them initially at purities known to be greater than 95 %. Thus it is reasonable to expect that a few percent of the Mössbauer absorption in the experimental spectra may be due to the other iron-containing species, possibly inactive forms of ferredoxin, and thus exact fit is not expected.

In the reduced state, the plant-type ferredoxins exhibit Mössbauer spectra characteristic of two quadrupole pairs at high temperatures. One quadrupole pair (iron site No. 2) is characteristic of high-spin ferrous iron[20,22] with a large quadrupole splitting (approx. 3.00 mm/sec) and a relatively large isomer shift (I.S./Pt = +0.2 mm/sec). The other quadrupole pair (iron site No. 1) is almost identical to those shown by the oxidized proteins and will be shown later to be attributable to a high

spin ferric atom. This double quadrupole pair interpretation is ascertained by the computer fitting of the high temperature data at 46 kGauss applied magnetic field (Fig. 6). The computer fit also gives the sign of the major component of the electric field gradient tensor as negative at the ferrous iron, although this assignment is only marginally preferred over a positive sign for this parameter. However, the fits shown in Figs. 7 and 8 for the low-temperature spectra in spinach and parsley ferredoxins will allow an unambiguous assignment of the parameters, employing the A-values measured by ENDOR. Table II lists the Mössbauer parameters for the high temperature (approx. 250°K), low-field data on the reduced forms of the proteins as well as the transition temperature at which the spectrum is composed of equal parts of the high-temperature and low-temperature contributions (*cf.* Fig. 4).

Figs. 7A, 7B and 7C show a comparison between the experimental spectra for reduced spinach ferredoxin at 4° K and 580 Gauss and best fits generated by computer simulation. Fig. 7A is the computed spectrum for the Fe(III) atoms including both the spin-up and spin-down states of the resultant electronic spin, since the applied field is very small in comparison to the hyperfine field and hence the spectra for the two electronic states are nearly identical. Fig. 7B is the computed spectrum for the Fe(II) atoms including both the spin-up and spin-down states for the $S = 1/2$ resultant

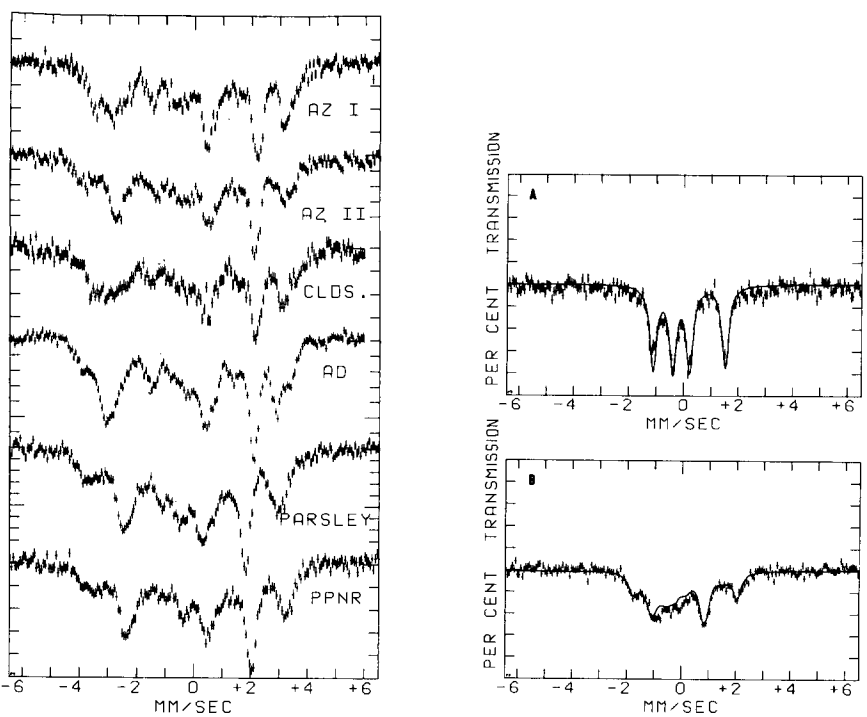

Fig. 5. Mössbauer spectra of the reduced proteins at 4°K and $H = 46$ kGauss; platinum source matrix; H parallel to the γ-ray direction. From top to bottem: Azotobacter protein I, Azotobacter protein II, Clostridium paramagnetic protein, adrenodoxin, parsley ferredoxin, spinach ferredoxin.

Fig. 6. Experimental (crosses) and calculated (solid line) Mössbauer spectra for reduced spinach ferredoxin at 256°K and (A) $H = 0$, and (B) $H = 46$ kGauss applied magnetic field parallel to the γ-ray direction; platinum source matrix.

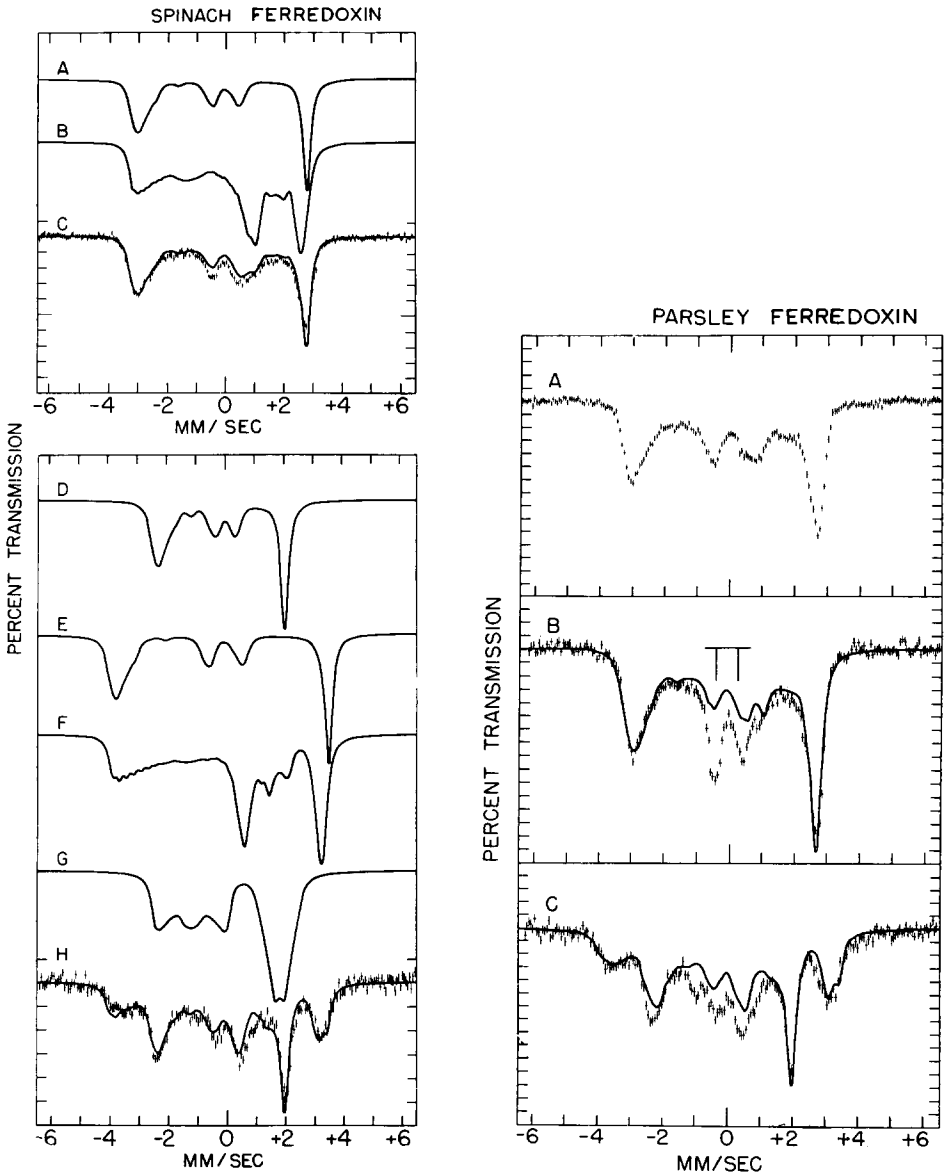

Fig. 7. Experimental (crosses) and calculated (solid lines) Mössbauer spectra for reduced spinach ferredoxin (lyophilyzed) at 4.2°K and with 580 Gauss (A–C) and 46 kGauss (D–H) applied fields parallel to γ-ray direction; platinum source matrix. (A) Ferric iron $m_s = \pm 1/2$; (B) ferrous iron $m_s = \pm 1/2$; (C) sum of A and B superimposed over experimental spectrum; (D) ferric; $m_s = -1/2$; (E) ferric: $m_s = 1/2$; (F) ferrous: $m_s = -1/2$; (G) ferrous: $m_s = 1/2$; (H) weighted sum of D, E, F and G superimposed over experimental spectrum (E and G are weighted 0.3 times the weights of D and F).

Fig. 8. Experimental (crosses) and calculated (solid lines) Mössbauer spectra for reduced parsley ferredoxin at 4.2°K and with 580 Gauss (A, B) and 46 kGauss (C) applied fields parallel to the γ-ray direction; platinum source matrix. The sample for B and C was the same showing oxidized signal indicated by the vertical lines in B and the sample for A was different, the latter showing little or no oxidized signal.

TABLE II

MÖSSBAUER PARAMETERS FOR THE REDUCED PROTEINS AT HIGH TEMPERATURES

The parameters are obtained from data taken at approximately 250°K in each case and the blanks indicate that no data is available.

Protein	*Ferric*		*Ferrous*		*Transition temp.* (°K)
	*I.S./Pt**	*Q.S.*	*I.S./Pt**	*Q.S.*	
Spinach ferredoxin	−0.06	0.64	+0.21	2.63	50
Parsley ferredoxin	−0.06	0.68	+0.23	2.77	60
Adrenodoxin	−0.07	0.81	+0.19	2.72	100
Azotobacter iron-sulfur protein I	—	—	—	—	100
Azotobacter iron-sulfur protein II	—	—	—	—	
Clostridium paramagnetic protein	—	—	—	—	100

* Isomer shifts (mm/sec) given relative to ^{57}Co:Pt source; values accurate to ± 0.02 mm/sec.

electronic spin and Fig. 7C displays the sum of Figs. 7A and 7B as compared to the experimental data.

Figs. 7D through 7H present a similar comparison for data on the same protein at 4°K but with a 46-kGauss magnetic field present. Here the spectra resulting from the relatively long-lived net electronic spin-up and spin-down states are significantly different because the applied field is comparable to the hyperfine field produced by the electrons at the nucleus and these two spectra must be weighted by the appropriate Boltzmann population ratio of the two electronic states (exp $-g\beta H/kT$). The slight anisotropy in g may be neglected since it has negligible effect on the populations. Fig. 7D displays the computer-simulated spectra for Fe(III) atoms in molecules with the electron spin antiparallel to the applied magnetic field (for these atoms, which have a negative effective hyperfine tensor, the hyperfine field produced at the nucleus is antiparallel to the applied field; hence a smaller overall magnetic splitting results). Fig. 7E displays the computed spectra for Fe(III) atoms in molecules with the electron spin parallel to the applied field (and hence the hyperfine field is directed parallel to the applied field resulting in a larger overall magnetic splitting). These two spectra must have their areas weighted by the electronic Boltzmann factor for the respective states; thus the spectrum in Fig. 7D (for the ground electronic state) is weighted more than that in Fig. 7E. Fig. 7F displays the computed spectrum for Fe(II) atoms in molecules with the net electron spin antiparallel to the applied magnetic field and Fig. 7G, the computed spectrum for Fe(II) atoms in molecules with the net electron spin parallel to the applied magnetic field. This latter spectrum results when the total effective magnetic field at the nucleus gives a Zeeman splitting which is small or comparable to the quadrupole splitting and $|\eta| > 0$[20,22]. This is just indicative of the smaller effective hyperfine tensor and the large electric field gradient tensor for the Fe(II) atom in these proteins. These latter two spectra must also have their areas weighted by the respective electron Boltzmann factors in the applied magnetic field. All four spectra are then added, using the weighting discussed above and the result compared to the experimental data in Fig. 7H. The agreement between theory and experiment is extremely good. It should be emphasized at this point that this is a four parameter fit (A_x, A_y, Q.S. and η for ferrous), the other parameters being fixed by the ENDOR experiments and high temperature Mössbauer

fits (Fig. 6). The uniqueness of these four parameters is discussed at the end of this paper. It may be seen that the spectrum in Fig. 7F must be weighted more than the spectrum in Fig. 7G thereby identifying the former as being due to the electronic ground $m_s = -1/2$ state (electron spin antiparallel to the applied field). Notice that for this state in the ferric atom (Fig. 7D) the hyperfine field was antiparallel to the applied field but for the same electron state in the ferrous atom (Fig. 7F) the hyperfine field is parallel to the applied field (resulting in a larger overall splitting) thus showing that the effective hyperfine tensor for the ferrous atom must be positive, opposite to that for the ferric atom. This can only be true if the two atoms are antiferromagnetically coupled as will be seen in the discussion to follow.

It was feared that the Kapitza resistance[24] of ice might cause the frozen aqueous samples to have a temperature higher than that registered by the carbon resistor when at helium temperatures. Because this would add still another parameter that would need to be determined by a computer fit, the spinach ferredoxin and adrenodoxin samples were lyophilized. The spectra from these lyophilized samples proved to be the same as those from the proteins in frozen aqueous solutions for all temperatures employed in this study.

Fig. 8 displays similar fits for parsley ferredoxin. Figs. 8A and 8B show the experimental data obtained for two different samples of parsley ferredoxin in applied magnetic fields of 580 Gauss. The difference between these two spectra is in the large doublet in Fig. 8B and is attributed to oxidized protein inasmuch as the oxidized

TABLE III

MÖSSBAUER PARAMETERS FOR THE REDUCED PARSLEY AND SPINACH FERREDOXINS AT 4.2°K

Both the effective A-tensor components ($A_{x,y,z}'$) and the actual atomic A-tensor components ($A_{x,y,z}$) are expressed in MHz (1 MHz = $3.34 \cdot 10^{-5}$ cm^{-1}) for the ground ($I = 1/2$) state of ^{57}Fe. The numbers in parentheses are equivalent gauss at the electron.

Mössbauer parameter	*Parsley*		*Spinach*	
	Ferric	*Ferrous*	*Ferric*	*Ferrous*
I.S./Pt (mm/sec)	-0.10 ± 0.02	$+0.19 \pm 0.02$	-0.10 ± 0.02	$+0.19 \pm 0.02$
Q.S. (mm/sec)	$+0.68 \pm 0.02$	-3.00 ± 0.1	$+0.64 \pm 0.02$	-3.00 ± 0.1
η	-0.9 ± 0.3	0 ± 0.2	-0.6 ± 0.3	0 ± 0.2
A_x' (MHz)	-51 ± 1*	11.2 ± 5.5	-51 ± 1*	11.1 ± 5.5
(G)	(-19.3 ± 0.4)*	4.2 ± 2	-19.4 ± 0.4*	4.2 ± 2
A_y' (MHz)	-46.2 ± 3	14 ± 5.6	-49.1 ± 2.5	16.8 ± 5.5
(G)	(-16.9 ± 1.1)	5.1 ± 2	-17.9 ± 0.8	6.1 ± 2
A_z' (MHz)	-42 ± 2*	$33.6 \pm 3.4 / -1.6$*	-42 ± 1.5*	35.3 ± 2*
(G)	(-14.7 ± 0.7)*	$11.7 \pm 1.3 / -0.5$*	-14.7 ± 0.4*	12.3 ± 0.7*
G_x	1.90		1.89	
G_y	1.96		1.96	
G_z	2.05		2.05	
A_x (MHz)	-21.9	-8.4	-21.9	-8.3
A_y (MHz)	-19.8	-10.5	-21.0	-12.6
A_z (MHz)	-18	-25.2	-18	-26.5

* Errors imposed by ENDOR measurements[9].

spectrum is at exactly the same place as indicated by the two vertical bars in Fig. 8B. This is included to show what can happen in the middle of the spectrum and hence that a good fit in the middle of the spectrum is not to be demanded in fitting Mössbauer data from labile proteins, particularly at low applied magnetic fields. Fig. 8B shows the computed spectrum (without oxidized material added) resulting from the parameters in Table III; notice that this is a reasonably good fit to the spectrum in Fig. 8A, but because of the oxidized material in the second sample, it does not fit the middle region of Fig. 8B. On the other hand, if a large magnetic field (46 kGauss) is applied to the sample of Fig. 8B, the spectrum in Fig. 8C is obtained. Fig. 8C also displays the computed spectrum (ignoring oxidized material) using the parameters in Table III; notice that the agreement in the middle of the spectrum is now better due to the fact that the spectrum of the oxidized material is now spread out and hence is now a smaller percentage of the absorption at any given velocity. The parameters which resulted from the computer fits are shown in Table III. This table includes the information available from ENDOR experiments[9]; namely, the magnitudes of the major components of the effective A-tensor at the ferric site and the magnitude of the z-component of the effective A-tensor at the ferrous site. These parameters were considered fixed within the errors allowed by the ENDOR measurements and were essential in obtaining a unique fit to the Mössbauer spectra. The parameter tolerances in Table III result from a trial and error approach to fitting curves to the experimental data.

DISCUSSION

The Mössbauer spectra obtained in this study are in agreement with those previously obtained for the oxidized forms of the proteins[25–28]. For the reduced proteins, previous investigations have yielded widely differing spectra. The 4.2°K spectra published by MOSS *et al.*[25,27] and by JOHNSON *et al.*[26] show a quadrupole pair of lines in the reduced form which is indicative of high-spin Fe(II) along with a pair of lines consistent with high-spin Fe(III) without hyperfine splitting. At least in the work of Moss *et al.*[25,27] it is now believed that this type of spectrum resulted from denaturation of the protein sample; in the current studies this spectral artifact could also be obtained; however, the denatured protein (avoided by more careful buffering) did not display the "$g = 1.94$" EPR signal which has been taken as a physical assay for the proper reduced state of the protein. Recent experimental work by JOHNSON *et al.*[29] and RAO *et al.*[30] are consistent with that reported here. It should be emphasized, however, that because no computer simulations were performed by these authors, several spectral lines which are due to Fe(III) were assigned mistakenly to Fe(II) (*cf.* Fig. 4 of ref. 29 and 30), and hence these authors were led to the erroneous conclusion that the effective hyperfine field for Fe(II) was nearly the same as for Fe(III). In fact, these fields are grossly different as is revealed by Table III. The conclusion drawn by the above authors that the iron atoms are antiferromagnetically coupled is, in our opinion, correct but the argument presented to support this conclusion is not for the following reasons. The two sets of stick spectra[29,30] indicated as arising from effective fields of $|H_1^n - H|$ and $|H_2^n + H|$ are actually due to the two effective fields at the Fe(III) site alone, caused by the two spin states of the total electron spin ($S = 1/2$) which cause the hyperfine field to add and subtract respectively from

the applied magnetic field at the Fe(III) site. This may be seen from the fact that an equally good stick spectral fit may be obtained by assuming that both isomer shifts, quadrupole splittings and magnitudes of the hyperfine fields are identical and equal to those attributed to ferric — a strong indication that these lines are arising from a single atom with just the net electronic spin projection reversed. The interpretation offered by JOHNSON *et al.*[29] and RAO *et al.*[30] is not only in direct contradiction to theory which predicts a highly anisotropic hyperfine tensor and a large quadrupole splitting for the high-spin Fe(II) atom[20,22], but also is in direct contradiction to their own data; *e.g.* the high-temperature data in Fig. 4 of ref. 30 shows that the quadrupole splitting for the Fe(II) atom is indeed large (contrary to their stick spectra) and the low-temperature spectra in Fig. 5 of ref. 30 shows that the lines at 4.2°K occurring at approx. −1.5 and −3.1 mm/sec and attributed to the ground electronic state of the Fe(II) atom by these authors have in fact nearly disappeared in the 1.7°K spectrum, thus indicating that they are from an excited electronic state (Fe(III), as we indicate) instead. The fact that the lines at positive velocity persist at 1.7°K indicates that the spectrum for the ground electronic state of Fe(II) has lines at positive velocity (which is true), but it has no resolved lines at negative velocity, contrary to these authors' stick spectra. Hence the conclusion that the hyperfine field at the ferric atom is the same as that at the ferrous atom is incorrect, because these authors have determined the hyperfine field for only a single atom, the Fe(III) atom; likewise the conclusion that these spectra demonstrate antiferromagnetic spin coupling at the two iron sites wherein the hyperfine field at one atom is opposite that at the other is unwarranted because they have never determined the other hyperfine field. The top and bottom stick spectra which they show (*cf.* Fig. 4, refs. 29 and 30) are, in fact, from a single atom with the total electron spin up and down, respectively, and simply serve to verify that the total electronic spin is one-half and do not verify antiferromagnetic coupling between atoms as was contended. To make the latter conclusion it is necessary to substract the ferric Mössbauer spectra by computer simulation and look at what is left, which will be due to the ferrous atom. This is effectively what was done in this paper and the conclusions in regard to the sign of A at the ferrous site being opposite that for the ferric site (and hence indicating antiferromagnetic coupling between the two atoms) come from computer simulations of the resulting ferrous spectra as indicated in Fig.7. This latter procedure was not followed by the above authors and hence it would appear that they may not draw any conclusions in regard to the spin coupling of the two atoms (since they have discerned only the spectrum from the ferric atom) except insofar as the total electronic spin is one half, a fact which was established earlier from EPR and susceptibility measurements.

The small quadrupole splitting (approx. 0.7 mm/sec) observed for the oxidized states of these proteins, again in accordance with the work by MOSS *et al.*[25,27], is consistent with all of the iron in the oxidized form of the protein being high-spin ferric (a conclusion reached later in this discussion), the observed quadrupole splitting coming from the ligands as the spherical symmetry of a free Fe(III) $3d^5$ electronic configuration would produce no quadrupole splitting.

The first finding from our analysis of the Mössbauer data is that the two iron atoms in the plant-type iron–sulfur proteins are spin-coupled in both the oxdized and the reduced forms of the proteins. This argument proceeds as follows: the quadru-

pole parameters for iron at Site 2 in the reduced form of the proteins show that this site is high-spin ferrous (*i.e.* $S = 2$). The positive effective A-values for this site are conclusive evidence for the presence of an antiferromagnetic exchange interaction with a spin greater than two: the A-values of high-spin iron compounds with a single iron atom are always negative[20]. Thus, only in the case of spin-coupling with a spin greater than two can the magnetic moment of the ferrous atom be oriented opposite to the resultant magnetic moment of the system, thereby reversing the sign of the effective A-values for the ferrous iron. Since $S = 5/2$ is the largest spin available, iron at site No. 1 is necessarily high-spin ferric.

Because the reduced form of the proteins contain a high-spin ferric spin-coupled to a high-spin ferrous, we then conclude that the oxidized proteins contain two high-spin ferric atoms spin-coupled to give a resultant diamagnetism to the complex. This conclusion is supported in the values of I.S. and Q.S. for the iron site No. 1, which match very well the parameters for the oxidized proteins. This would seem to indicate that the iron in the oxidized proteins is also high-spin ferric. The diamagnetism at iron sites in the oxidized proteins must result therefore from a negative exchange-coupling constant between the electron spins at the two iron sites. This conclusion is confirmed by magnetic susceptibility measurements[10,11].

An indication of the physics involved in the calculation and interpretation of the Mössbauer spectra resulting from two spin-coupled iron atoms may be seen by considering an idealized situation where the G- and A-tensors are isotropic and ∇E is zero. In the reduced state, the electron spin ground state wave function is given in terms of vector coupling of the spin states 5/2 and 2 to give a resultant spin 1/2. For this wave function (ψ):

$$\begin{aligned}
&\langle\psi| -\beta\tilde{S}_1\cdot\overset{=}{G}_1\cdot\tilde{H} - \beta\tilde{S}_2\cdot\overset{=}{G}_2\cdot\tilde{H} + \tilde{I}_1\cdot\overset{=}{A}_1\cdot\tilde{S}_1 + \tilde{I}_2\cdot\overset{=}{A}_2\tilde{S}_2 - g_n\beta_n\tilde{I}_1\cdot\tilde{H} - g_n\beta_n\tilde{I}_2\cdot\tilde{H}\,|\psi\rangle \\
&= +m_s\left(\frac{7}{3}g_1 - \frac{4}{3}g_2\right)\beta H + m_s\frac{7}{3}A_1m_{I_1} - m_s\frac{4}{3}A_2m_{I_2} - g_n\beta_nm_{I_1}H - g_n\beta_nm_{I_2}H \\
&= +m_sg\beta H + A_1'm_sm_{I_1} + A_2'm_sm_{I_2} - g_n\beta_nm_{I_1}H - g_n\beta_nm_{I_2}H \qquad (3)
\end{aligned}$$

where m_s is the projection of $S = S_1 + S_2$ on H, *i.e.* $\pm 1/2$. A_1 and A_2 are the actual hyperfine tensors for the individual atoms, $\overset{=}{G}_1$ and $\overset{=}{G}_2$ are the individual atom G-tensors, g_1 and g_2 are the components of the isotropic G-tensors, A_1 and A_2 are the components of the actual hyperfine tensors for the individual atoms, A_1' and A_2' are the components of the effective hyperfine interactions which are measured by Mössbauer spectroscopy, g_n is the nuclear g-factor, I_1 and I_2 are the projections of these nuclear spins along H. Note that the sign of the effective hyperfine interaction is reversed at iron site No. 2 ($A_2' = -{}^4/_3A_2$), a reversal which is also indicated by the data shown in Fig. 7. This reversal is a direct consequence of the antiferromagnetic coupling between the two iron atoms as shown in Eqn. 3.

Eqn. 3 may be rewritten in terms of effective hyperfine fields at the nuclei as follows:

$$E = +m_sg\beta H - g_n\beta_nm_{I_1}\left(H - \frac{A_1'm_s}{g_n\beta_n}\right) - g_n\beta_nm_{I_2}\left(H - \frac{A_2'm_s}{g_n\beta_n}\right) \qquad (4)$$

where the quantities in parentheses can be considered as effective magnetic fields at the nuclei. These are the effective fields referred to by JOHNSON *et al.*[29] and RAO

et al.[30]. Notice that for each iron atom there are two values of m_s and hence two different effective fields corresponding to $|H - H_n|$ and $|H + H_n|$ where $H_n = A'/2g_n\beta_n$ = effective hyperfine field produced at the nucleus by the electron. These are the two fields which the above authors[29,30] have observed for ferric and have nothing to do with the hyperfine field at the second iron site (Fe(II)).

The above treatment is a good approximation for the ferric atom (iron site No. 1) where the hyperfine tensor is nearly isotropic and the quadrupole interaction is small; however, for the ferrous atom the above approximation is very poor and a more complicated expression which accounts for the anisotropies in $\tilde{G}$, $\tilde{A}$ and $\tilde{\tilde{\nabla E}}$ is needed. This more complicated expression adds nothing to the discussion of the effect of spin-coupling presented here and will be omitted in this paper.

Assuming that the computer fits are unique, the quadrupole tensor at the Fe(II) site in spinach and parsley is uniquely characteristic of a single electron in a d_z^2 orbital (or a high-spin d^6 with d_z^2 lying low)[20,22]; the A-tensor for this site also shows the effect of the dipolar terms which would result from a high-spin d^6 configuration with d_z^2 lying low[20,22]. This may be seen by first obtaining the actual hyperfine tensors at the ferric and ferrous atoms using the relations $A_1 = \frac{3}{7}A_1'$ and $A_2 = -\frac{3}{4}A_2'$ shown in Eqn. 4. The results are listed in Table III. The actual A-tensor at the ferrous atom is approximately axial with the largest component along the z-axis, again indicating that the sixth electron is in the d_z^2 orbital[20,22].

The g-values for the reduced proteins are near $g = 2.002$, the free electron g-value. The d_{xz} and d_{yz} orbitals must be far above the d_z^2 orbital in order to obviate the large deviations from $g = 2.002$ which would result from the spin-orbit coupling between the d_z^2 orbital and the d_{xz} and d_{yz} orbitals. This arrangement of the d-orbitals implies a field which is more nearly tetrahedral or square-planar than octahedral; therefore, one can except $d_{x^2-y^2}$ to be somewhat closer to d_z^2 than the t-orbitals. In order to explain the observed temperature dependence of the Q.S. for iron site No. 2 in the reduced state, the lowest $d_{x^2-y^2}$ orbital must be around 500 cm^{-1} above the lowest d_z^2 orbital. We note here that the position of the $d_{x^2-y^2}$ orbital has been measured to be as large as 470 cm^{-1} above the lowest d_z^2 for a high-spin ferrous compound in a tetrahedral field[31].

It should be emphasized that this description of the states of the iron in these proteins follows directly from the data. Among previously proposed models, that put forth by GIBSON *et al.*[32] and THORNLEY *et al.*[33] comes closest to agreeing with our results. However, it is important to note that their model was put forward utilizing a crystal field approximation to account for the g-values of reduced spinach ferredoxin. The experimental Mössbauer parameters give information on the degree of covalency at the iron sites, and thus we have here a means to check the validity of the crystal field approximation with respect to the iron–sulfur complex in the plant-type ferredoxins. We compare the magnitudes of the A-values obtained by this study (Eqn. 3) with those calculated for the free ion by WATSON AND FREEMAN[34] using extended Hartree–Fock calculations. We find that the isotropic parts of the A-values at these iron sites are approximately one half that of the free ions; therefore these iron sites are covalent in accord with studies of ferric ions in zinc sulfide[35]. In addition, the A-values at the ferric iron sites exhibit anisotropies which are strictly forbidden for an S-state ion. These anisotropies cannot be explained by a crystal field treatment of this complex. Any explanation of the A- or G-tensors based

on crystal field approximations can be considered only fortuitously correct since sulfur ligands cause sizable spin-orbit contributions to the tensors which must be included. Thus, in the above discussion our use of *d*-orbitals must be interpreted as a gross approximation to the metallic contribution to the covalent orbitals actually present and the conclusion that d_{z^2} is the ground state at the ferrous site must be based primarily on considerations of the quadrupole tensor at this site. The low-lying $d_{x^2-y^2}$ orbital must be included in any calculation of the temperature-dependent susceptibility as is done in Paper III[10,11].

CONCLUSIONS

The following conclusions arise directly from the results of the experiments described and apply to all of the proteins in this study:

1. The oxidized forms of the plant-type iron–sulfur proteins contain two iron atoms, each is in the high-spin ferric form and they are coupled antiferromagnetically (presumably through a bridging ligand) to yield a diamagnetic complex at low temperatures.

2. The reduced forms of the proteins contain one high-spin ferric site (presumably identical to either site in the oxidized form of the protein) and a high-spin ferrous site; these sites are again antiferromagnetically coupled giving in this case a resultant electronic spin of 1/2 for the molecule in the ground state.

3. The iron bonding at all sites is covalent – a fact consistent with the known presence of sulfur as a ligand in the active site complex.

4. The large value of the quadrupole splitting of Fe(II) (3mm/sec) indicates that the ground electronic state is orbitally non-degenerate; the temperature dependence of the quadrupole splitting indicates that the first excited state lies at least 500 cm^{-1} above the ground state.

5. The values of the quadrupole parameters (large quadrupole splitting and small η) suggest tetrahedral symmetry about the iron in all sites; octahedral symmetry is certainly excluded.

In addition to the above, we conclude that at least in the case of spinach and parsley ferredoxins, the ferrous iron has an electronic ground state with d_{z^2} symmetry. The first excited state ($d_{x^2-y^2}$) is only 500 cm^{-1} above the ground state, thus, the ligand configuration at the ferrous site in these proteins is a distorted tetrahedron. The proof of this last conclusion (d_{z^2} symmetry) depends intimately on the uniqueness of the Mössbauer parameters at the ferrous site. A rigorous proof of uniqueness for these parameters is contingent on the determination of A_x and A_y for this site by ENDOR experiments. These experiments are presently under way. In the case of adrenodoxin, further Mössbauer spectroscopic experiments are planned which hopefully will allow a choice between the possible symmetries at the ferrous site: *e.g.* between square planar and tetrahedral ligand symmetry.

ACKNOWLEDGMENTS

This work has been carried out under grants-in-aid from the National Science Foundation (GB-13585) and the biology and medicine program of the U. S. Atomic Energy Commission through Donner Laboratory, and from the National Institutes

of Health (GM-12176, GM-12394, and RR-00417-01). One of the authors (W.R.D.) acknowledges predoctoral fellowship support through the Biochemistry Training Grant (2-TO1-GM-01045-06) to the Department of Chemistry, University of California, San Diego and another author (I.T.S.) through the National Institutes of Health Biophysics Training Grant (GM-1355) to the Biophysics Research Division, University of Michigan; we also acknowledge the partial support provided by a Public Health Service Research Career Award to H.B (5-KO6-GM-18,442) and by Public Health Service Research Career Development Awards to A.J.B. (1-K4-GM-24,494), G. P. (1-K3-GM-21,213) and W.H.O-J (1-K3-GM-10,236). We are grateful to Drs. D. V. DerVartanian and Y. I. Shethna for samples of the Azotobacter proteins to Dr. R. W. F. Hardy for *Clostridium pasteurianum* cells, and to Dr. D. O. Hall for sending us a preprint of his recent work[30] prior to publication. We have had valuable discussions during the course of this work with Drs. I. C. Gunsalus, R. G. Bartsch and G. Lang. We are particularly grateful to Dr. G. Lang for furnishing us with output from his own spectral synthesis program as a check on the one employed here. Finally, we acknowledge the creative technical support provided by Charles N. Bartlett.

REFERENCES

1 B. B. BUCHANAN, *Struct. Bonding*, 1, (1966) 3.
2 R. MALKIN AND J. C. RABINOWITZ, *Ann. Rev. Biochem.*, 36 (1967) 113.
3 D. O. HALL AND M. C. W. EVANS, *Nature*, 223 (1969) 1342.
4 Y. I. SHETHNA, P. W. WILSON, R. E. HANSEN AND H. BEINERT, *Proc. Natl. Acad. Sci. U.S.*, 52 (1964) 1263.
5 G. PALMER, *Biochem. Biophys. Res. Commun.*, 27 (1967) 315.
6 H. BEINERT AND W. H. ORME-JOHNSON, *Ann. N. Y. Acad. Sci.*, 158 (1969) 336.
7 W. H. ORME-JOHNSON, R. E. HANSON, H. BEINERT, J. C. M. TSIBRIS, R. C. BARTHOLOMAUS AND I. C. GUNSALUS, *Proc. Natl. Acad. Sci. U.S.*, 60 (1968) 368.
8 J. C. M. TSIBRIS, R. L. TSAI, I. C. GUNSALUS, W. H. ORME-JOHNSON, R. E. HANSON AND H. BEINERT, *Proc. Natl. Acad. Sci. U.S.*, 59 (1968) 959.
9 J. FRITZ, R. ANDERSON, J. A. FEE, G. PALMER, R. H. SANDS, J. C. M. TSIBRIS, I. C. GUNSALUS, W. H. ORME-JOHNSON AND H. BEINERT, *Biochim. Biophys. Acta*, 253 (1971) 110.
10 G. PALMER, W. R. DUNHAM, J. A. FEE, R. H. SANDS, T. IIZUKA AND T. YONETANI, *Biochim. Biophys. Acta*, 245 (1971) 201.
11 T. KIMURA, A. TASAKI AND H. WATARI, *J. Biol. Chem.*, 245 (1970) 4450.
12 W. EATON, G. PALMER, J. A. FEE, T. KIMURA AND W. LOVENBERG, *Proc. Natl. Acad. Sci. U.S.*, submitted.
13 D. V. DERVARTANIAN, Y. I. SHETHNA AND H. BEINERT, *Biochim. Biophys. Acta*, 194 (1969) 548.
14 R. W. F. HARDY, E. KNIGHT, JR., C. C. MACDONALD AND A. J. D'EUSTACHIA, in A. SAN PIETRO, *Non-Heme Iron Proteins: Role in Energy Conversion*, Antioch Press, Yellow Springs Ohio, 1965, p. 275.
15 W. H. ORME-JOHNSON AND H. BEINERT, *J. Biol. Chem.*, 244 (1969) 6143.
16 G. PALMER, *Biochem. Biophys. Res. Commun.*, 27 (1967) 315.
17 J. A. FEE, AND G. PALMER, *Biochim. Biophys. Acta*, 245 (1971) 175.
18 H. BEINERT, in W. LOVENBERG, *Iron-Sulfur Proteins*, Academic Press, New York, in the press.
19 S. G. MAYHEW, D. PETERING, G. PALMER AND G. P. FOUST, *J. Biol. Chem.*, 244 (1969) 2830.
20 W. R. DUNHAM, Ph. D. Thesis, University Microfilms, Ann Arbor, Mich., 1970, Order No. 70-19, 588.
21 A. J. BEARDEN, M. G. HAUSER AND P. L. MATTERN, *Mössbauer Effect Methodol.*, 1 (1965) 67.
22 G. LANG, *Q. Rev. Biophys.*, 3 (1970) 1.
23 V. I. GOLDANSKII AND E. F. MAKAROV, in V. I. GOLDANSKII AND R. H. HERBER, *Chemical Applications of Mössbauer Spectroscopy*, Academic Press, New York, 1968, p. 23.
24 G. L. POLLACK, *Rev. Mod. Phys.*, 41 (1968) 48.
25 A. J. BEARDEN AND T. H. MOSS, in A. EHRENBERG, B. G. MALMSTROM AND T. VANNGARD, *Magnetic Resonance in Biological Systems*, Pergamon Press, London, 1967, p. 391.
26 C. E. JOHNSON AND D. O. HALL, *Nature*, 217 (1968) 446.
27 T. H. MOSS, A. J. BEARDEN, M. A. CUSANOVICH, R. G. BARTSCH AND A. SAN PIETRO, *Biochemistry*, 7 (1968) 1591.

28 C. E. JOHNSON, E. ELSTNER, J. F. GIBSON, G. BENFIELD, M. C. W. EVANS AND D. O. HALL, *Nature*, 220 (1968) 1291.
29 C. E. JOHNSON, *Phys. Today*, 24 No. 2, (1971) 35.
30 K. RAO, K. R. CAMMACK, D. O. HALL AND C. E. JOHNSON, *Biochem. J.*, 122 (1971) 257.
31 P. R. EDWARDS, C. E. JOHNSON, AND R. J. P. WILLIAMS, *J. Chem. Phys.*, 47 (1967) 2074.
32 J. F. GIBSON, D. O. HALL, J. H. M. THORNLEY AND F. R. WHATLEY, *Proc. Natl. Acad. Sci. U.S.* 56 (1966) 937.
33 J. H. M. THORNLEY, J. F. GIBSON, F. R. WHATLEY AND D. O. HALL, *Biochem. Biophys. Res. Commun.*, 24 (1966) 877.
34 R. E. WATSON AND A. J. FREEMAN, *Phys. Rev.*, 123 (1961) 2027.
35 R. S. TITLE, *Phys. Rev.*, 131 (1963) 623.